Sensing and Bio-Sensing Research 8 (2016) 59–64

Contents lists available at ScienceDirect

Sensing and Bio-Sensing Research

journal homepage: www.elsevier.com/locate/sbsr

Elution time changes due to anomalous DEP effects in microchannels under uniform and non-uniform electric fields

Antonino Magliano [a,*], Massimo Camarda [a,d], Salvatore Francesco Lombardo [a], Rossana Di Martino [c], Michele Cascio [a], Alessandra Romano [b], Luigi Minafra [c], Giorgio Russo [c], Mariacarla Gilardi [c], Francesco Di Raimondo [b], Silvia Scalese [a], Antonino La Magna [a]

[a] CNR-IMM Sezione di Catania, Z.I. VIII Strada 5, I-95121 Catania, Italy
[b] Divisione de Ematologia AOUP Vittorio Emanuele Catania, Italy
[c] IBFM-CNR, Cefalù, PA Sicilia, Italy
[d] Laboratory for Micro and Nanotechnology Paul Scherrer Institute, CH-5232, Villigen-PSI, Switzerland

ARTICLE INFO

Article history:
Received 31 August 2015
Accepted 14 February 2016

Keywords:
Dielectrophoresis
Anomalous DEP
Field flow fractionation
Cell diffusion

ABSTRACT

Conventional dielectrophoresis (DEP) force on cell and particle is altered in the proximity of the electrodes due to the failure of the dipole approximation. In these conditions an anomalous DEP (aDEP) force rules the particle manipulation. Anyhow, the role of the aDEP is barely considered in the design of DEP devices. Here we analyze, using a multiscale simulation approach, the aDEP effects in micro-fluidic device coupled with interdigitated channel commonly used in continuous mode field flow fractionation dielectrophoretic (FFF-DEP) devices for the separation of circulating tumor cells (MDA) and Lymphocytes (LYM). We study the propagation of an injected density of MDA and LYM respectively and evaluate how the aDEP changes the migrations of the cells.

1. Introduction

Dielectrophoresis (DEP) based techniques are nowadays routinely used to separate neutral micro- and nano-particles suspended on a liquid medium in micro-fluidic device. The techniques are based on the dielectrophoretic (DEP) force that derives from the induced polarization under a non-uniform electric field [1,2].

$$F_{DEP} = \left(\vec{p}\cdot\vec{\nabla}\right)\vec{E} \tag{1}$$

$$\vec{p} = 3V\varepsilon_m Re[f_{CM}(\omega)]\vec{E} \tag{2}$$

where $\vec{p}$, ε_m, V are respectively the induced dipole moment, the relative permittivity of the medium and the volume of the particle. The vector $\vec{E}$ is the external electric AC field imposed while f_{CM} is the so-called Clausius–Mossotti Factor:

$$f_{CM}(\omega) = \frac{\left(\tilde{\varepsilon}^{(p)} - \tilde{\varepsilon}^{(m)}\right)}{\left(\tilde{\varepsilon}^{(p)} + 2\tilde{\varepsilon}^{(m)}\right)} \tag{3}$$

with $\tilde{\varepsilon}^{(p)}, \tilde{\varepsilon}^{(m)}$ as the complex permittivities of the particles that depend on ε_0 (vacuum permittivity $8.85\cdot10^{-12}$ F/m) and σ (conductivity [S/m^2]) as shown below:

$$\tilde{\varepsilon}^{(j)} = \varepsilon_r^{(j)}\varepsilon_0 - i\frac{\sigma^{(j)}}{\omega}. \tag{4}$$

In particular, the dielectrophoretic force can be separated in two groups: negative DEP for $f_{CM} < 0$ (in this case the particles accelerate in the opposite direction of the vector $\nabla\vec{E}$ e.g. are pushed away from the electrodes inducing the field $\vec{E}$), positive DEP for $f_{CM}>0$ (in this case the particles are attracted by the electrodes). Indeed, using Eqs. (1)–(4) we derive the standard DEP force.

$$\vec{F}^{std}_{DEP} = 4\pi\varepsilon_m R^3 f_{CM}(\omega)\ \vec{\nabla}\vec{E}^2 \tag{5}$$

with R radius of the particle and $\vec{\nabla}\vec{E}^2$ the gradient of the square module of the imposed AC electric field and the sign of the force is equal to f_{CM}'s one.

The F_{DEP} using this approach (standard case) is not completely accurate since its validity depends on the validity of the dipole approximation Eq. (2). In a previous recent paper of our group we have studied the regime of the validity of (2) as a function of the distance between the particle and the electrodes. In this paper we have individuated the

Abbreviations: DEP, dielectrophoresis; FFF-DEP, field flow fractionation DEP; nDEP, negative-DEP; pDEP, positive-DEP; aDEP, anomalous DEP; MST, Maxwell Stress Tensor; MDA, human cancer cells mb — 231 triple negative; LYM, lymphocytes.

* Corresponding author.
E-mail address: maglianoantonino@gmail.com (A. Magliano).

http://dx.doi.org/10.1016/j.sbsr.2016.02.004

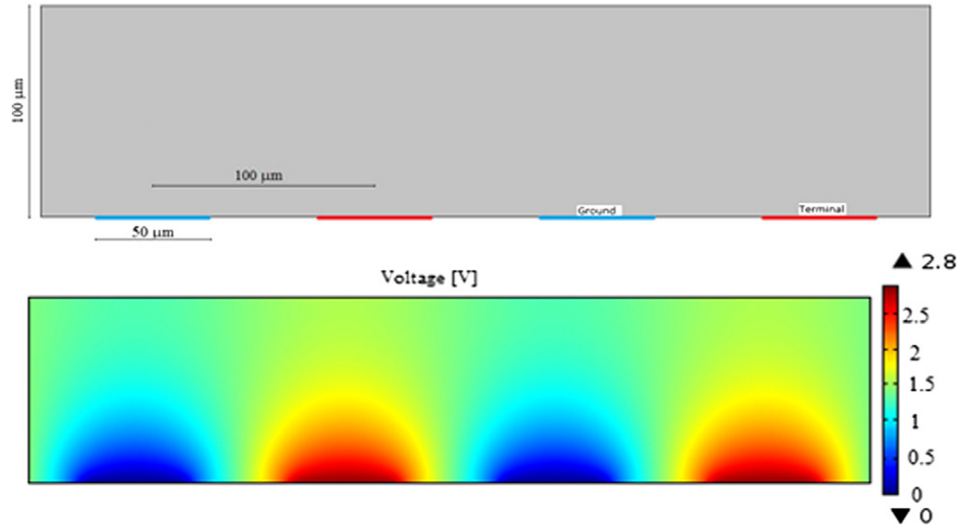

Fig. 1. Top graph: snapshots of the section of the interdigitated channel device. Bottom graph: calculated electric potential distribution.

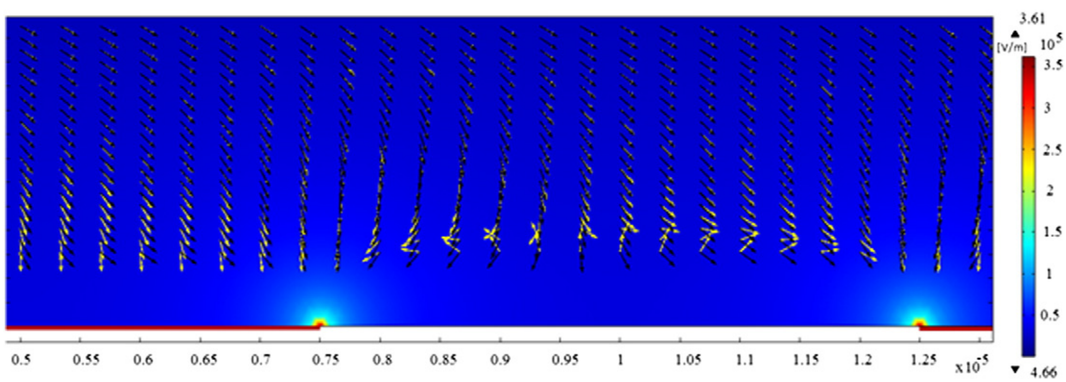

Fig. 2. DEP velocity field predicted for MDA by dipole approximation (black arrows) and MST (yellow arrows). It is possible to see how in the aDEP region the arrows change direction indicating a transition from attractive to repulsive regime. The aDEP region is located in the *center* between two consecutive electrodes.

geometric conditions that complicate the conventional scenario: the so-called anomalous DEP (aDEP) region of the device where particles with f_{CM}<0 are attracted by the electrodes (and vice-versa) and the general DEP response is altered. A generic approach for the theoretical study of the DEP interaction relies on the use of the Maxwell Stress Tensor (MST)

$$F_{DEP}^{MST} = \oint \overline{\overline{T}} \cdot \hat{n} dA \tag{6}$$

with Maxwell Stress Tensor $\overline{\overline{T}} = \varepsilon_m(E_iE_j - 0.5E_iE_j\delta_{ij})$ where E_i, E_j are the position dependent coordinates [4] of the electric field and the integration symbol indicates that the integral must be calculated in a region outside of the particle but infinitesimally close to its surface. The use of (6), although computationally expensive, avoids any approximation in the force calculation and in particular it evidences regions of repulsion where the common DEP predicts attraction in the case of nDEP. In the following sections, we report the numerical approach based on

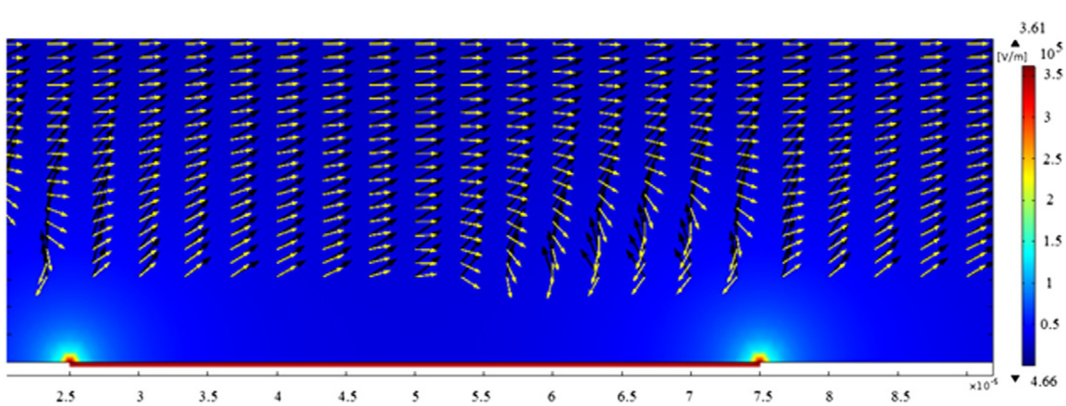

Fig. 3. DEP velocity field predicted for LYM by dipole approximation (black arrows) and MST (yellow arrows). It is possible to see how in the aDEP region the arrows change direction going from repulsive to attractive.

Fig. 4. Device with two different inlets for MDA case and LYM case.

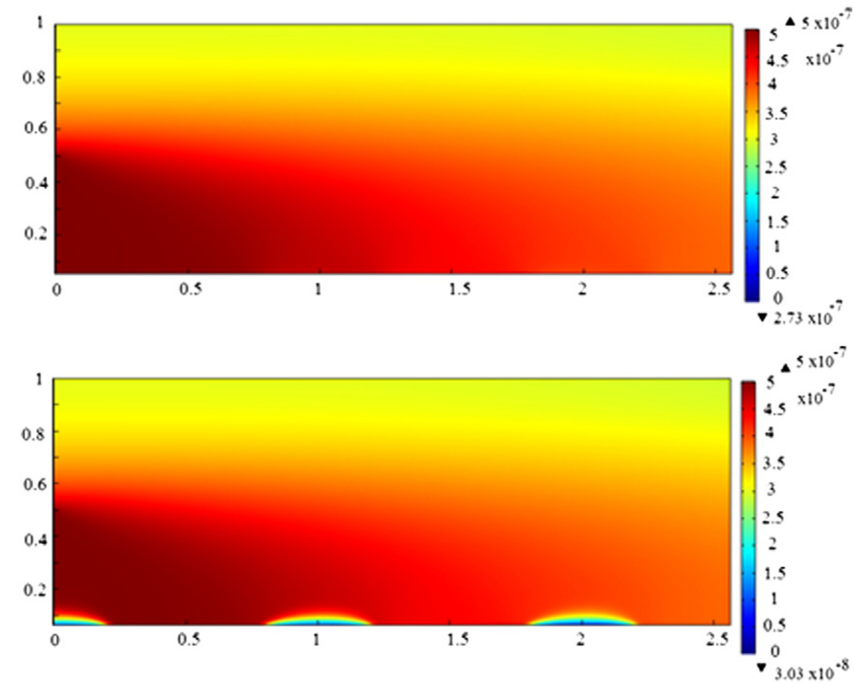

Fig. 5. Density field obtained by the drift–diffusion simulation for MDAs. In the top, we represent standard DEP results, in the bottom the results obtained with the MST method.

a drift–diffusion law for the migration of the cell, moreover we demonstrate by our simulation analysis the different predicted kinetics between standard DEP and aDEP for two different cell types.

2. Numerical approach

In order to perform our analysis in a realistic case we have considered the problem of the separation of the circulating tumor cells (in particular MDA — MB 231 triple negative breast cells) from lymphocytes (LYM). The calculation of the f_{CM} as a function of the frequency for two types of cells indicated that for the frequency of 60 kHz: MDA are subjected to pDEP while LYM to nDEP. As a consequence at this frequency we should efficiently separate the two branches of cell components in a mixed colloidal suspension of them. Unlike the standard DEP, aDEP is effective also in the presence of uniform electric field. As a consequence, a simple configuration where these effects can be easily evidenced is the planar capacitor which generates a uniform electric field and we can observe the aDEP contribution only [1]. However, our simulations were performed considering a realistic device geometry i.e. a channel with interdigitated electrodes as shown in Fig. 1 and an external non-uniform AC electric field IS imposed simulating the separation of particles at the indicated frequency of 60 kHz.

As it has been explained in the introduction, the particles are suspended in a liquid medium, which is assumed to flow through the channel velocity field $\vec{u}_{fluid}$ derived by the Navier–Stokes equation

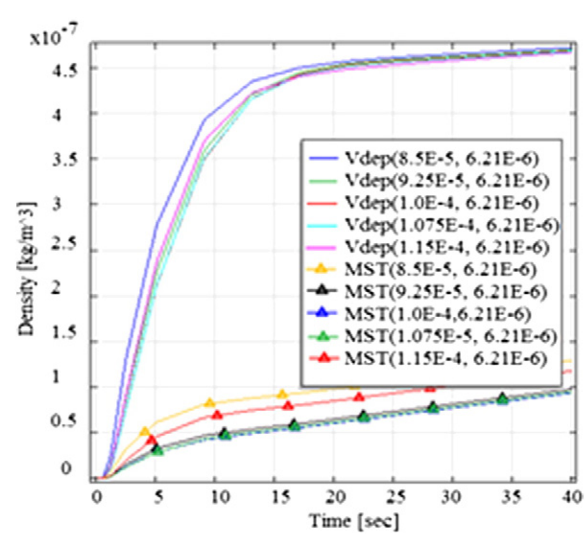

Fig. 6. Density as a function of the time for MDA case, in particular points located in the central region between two electrodes. MST and standard DEP results are compared.

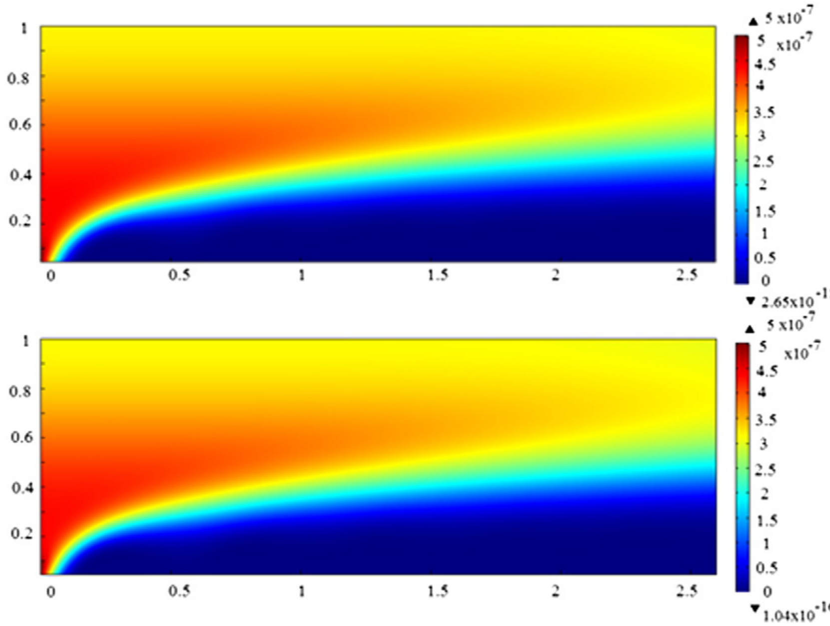

Fig. 7. Density field obtained by the drift–diffusion simulation for LYM cells. In the top, we represent standard DEP results, in the bottom the results obtained with the MST method.

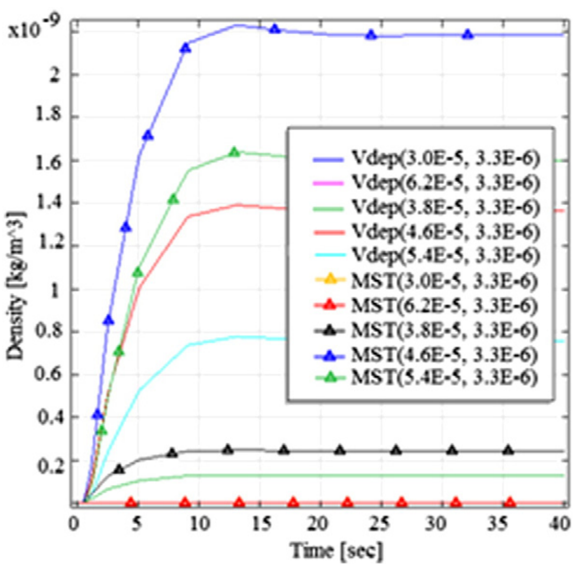

Fig. 8. Density as a function of the time for the LYM case, in particular points located in the central region of one electrode. MST and standard DEP results are compared.

(see below). In order to determinate the dielectrophoretic velocity of the particle in the reference system of the fluid (with the standard dipole approximation or with the MST method) we use the Stokes formula and the steady state relationships as shown below [3]:

$$F_{drag} = -f\vec{u} \tag{7}$$

$$F_{DEP} = -F_{drag} \tag{8}$$

$$u_{DEP} = \frac{F_{DEP}}{f} \tag{9}$$

where f is the friction factor that for the spherical particle became $6\pi\mu_{medium}R$, F_{drag} represents the flow resistance, and $\vec{u}$ is the velocity field. F_{DEP} can be determined numerically solving the Poisson equation

$$-\nabla\cdot\varepsilon\nabla V = 0 \leftrightarrow \vec{E} = -\nabla V \tag{10}$$

and using the two methods indicated in Section 1.

For the effective medium velocity $\vec{u}_{fluid}$ we need to solve the Navier–Stokes equation (with steady state and uncompressible condition (Eq. (10)))

$$\rho\left(\vec{u}_{fluid}\cdot\nabla\right)\vec{u}_{fluid} = -\nabla\rho + \eta\nabla^2\vec{u}_{fluid} + \vec{F} \tag{11}$$

with ρ indicating the density of the medium, η is the kinematic viscosity, $\vec{F}$ represents the generic vector of our study, ε is the electric permittivity, and $\vec{E}$ is the external electric field generated by the voltage V. The velocity field in the laboratory reference system is given by

$$u_{tot} = u_{fluid} + u_{DEP.} \tag{12}$$

Now, using this approach for standard approximation applying the formally correct MST method, we are able to determinate the aDEP region, comparing the differences between two methods.

This analysis is performed in Figs. 2 and 3 for MDA and LYM case respectively. In both figures we represent the velocity field (u_{tot}) starting from a distance from the electrodes equal to the particles' radii.

3. Drift–diffusion approach

In this section, we evaluate the anomalous DEP effects using a different approach to make evident the influence of the electrode proximity in the global cells' kinetics. We follow the motion of a given density of MDA and LYM entering from an inlet in an interdigitated channel device. We impose that particle density is governed by a drift–diffusion

Fig. 9. On the left side graphs the time dependent distribution of MDAs for the standard case (continuous line) and the MST forces is reported (line with triangle); on the right side graphs the same analysis is reported for LYMs.

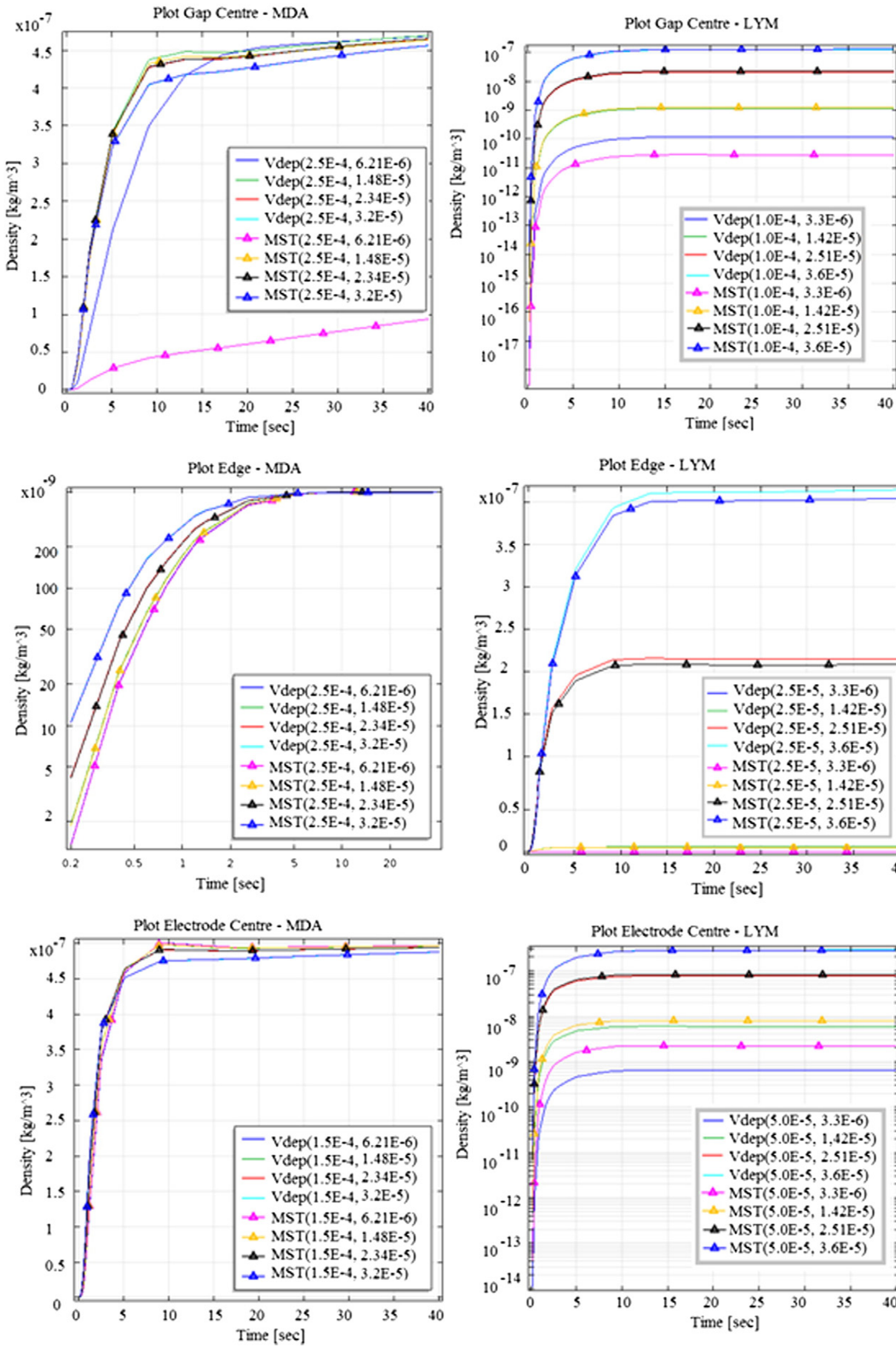
Plot Gap Centre - MDA
x10^-7
Density [kg/m^3]
Time [sec]
Vdep(2.5E-4, 6.21E-6)
Vdep(2.5E-4, 1.48E-5)
Vdep(2.5E-4, 2.34E-5)
Vdep(2.5E-4, 3.2E-5)
MST(2.5E-4, 6.21E-6)
MST(2.5E-4, 1.48E-5)
MST(2.5E-4, 2.34E-5)
MST(2.5E-4, 3.2E-5)
Plot Gap Centre - LYM
Density [kg/m^3]
Time [sec]
Vdep(1.0E-4, 3.3E-6)
Vdep(1.0E-4, 1.42E-5)
Vdep(1.0E-4, 2.51E-5)
Vdep(1.0E-4, 3.6E-5)
MST(1.0E-4, 3.3E-6)
MST(1.0E-4, 1.42E-5)
MST(1.0E-4, 2.51E-5)
MST(1.0E-4, 3.6E-5)
Plot Edge - MDA
x10^-9
Density [kg/m^3]
Time [sec]
Vdep(2.5E-4, 6.21E-6)
Vdep(2.5E-4, 1.48E-5)
Vdep(2.5E-4, 2.34E-5)
Vdep(2.5E-4, 3.2E-5)
MST(2.5E-4, 6.21E-6)
MST(2.5E-4, 1.48E-5)
MST(2.5E-4, 2.34E-5)
MST(2.5E-4, 3.2E-5)
Plot Edge - LYM
x10^-7
Density [kg/m^3]
Time [sec]
Vdep(2.5E-5, 3.3E-6)
Vdep(2.5E-5, 1.42E-5)
Vdep(2.5E-5, 2.51E-5)
Vdep(2.5E-5, 3.6E-5)
MST(2.5E-5, 3.3E-6)
MST(2.5E-5, 1.42E-5)
MST(2.5E-5, 2.51E-5)
MST(2.5E-5, 3.6E-5)
Plot Electrode Centre - MDA
x10^-7
Density [kg/m^3]
Time [sec]
Vdep(1.5E-4, 6.21E-6)
Vdep(1.5E-4, 1.48E-5)
Vdep(1.5E-4, 2.34E-5)
Vdep(1.5E-4, 3.2E-5)
MST(1.5E-4, 6.21E-6)
MST(1.5E-4, 1.48E-5)
MST(1.5E-4, 2.34E-5)
MST(1.5E-4, 3.2E-5)
Plot Electrode Centre - LYM
Density [kg/m^3]
Time [sec]
Vdep(5.0E-5, 3.3E-6)
Vdep(5.0E-5, 1,42E-5)
Vdep(5.0E-5, 2.51E-5)
Vdep(5.0E-5, 3.6E-5)
MST(5.0E-5, 3.3E-6)
MST(5.0E-5, 1.42E-5)
MST(5.0E-5, 2.51E-5)
MST(5.0E-5, 3.6E-5)

equation where the drift term is calculated by means of the Eqs. (1)–(12):

$$\frac{\partial \Phi}{\partial t} = -\vec{\nabla} \cdot \vec{J} \leftrightarrow \vec{J} = -D(\Phi)\nabla\Phi + \vec{u}_{tot}\Phi \quad (13)$$

with Φ as the particles' density, $\vec{J}$ the drift–diffusion current, $\vec{u}_{tot}$ is the total velocity field Eq. (12), and D(ϕ) represents the diffusion coefficient. In general, we can identify two terms: $\vec{u}_{tot}\Phi$ is the drift term while $D(\Phi)\nabla\Phi$ is the diffusion term [5,6].

To better evaluate the influence of aDEP effects for MDA and LYM motion in the colloidal solution, we introduce the particles in the channel from two different positions for the inlets as indicated in Fig. 4:

We have used two different positions to initialize the drift–diffusion equation due to the different responses of the cells to the DEP forces: MDAs positive DEP, determining an attraction to the electrodes and LYMs negative DEP, determining a repulsion from the electrodes).

4. Simulation results

As expected from the theory, in the aDEP zone we should have a different particle concentration space profile if the convection term is evaluated with the MST with respect to the standard method. In particular, we consider separately the two cases MDA and LYM and analyze in details the density field in the aDEP zones indicated in Figs. 2 and 3 (the working frequency 60 kHz is the same for both configurations).

The snapshots in Fig. 5 represent the MDAs and the time dependence of the density in particular points out of the aDEP zone is shown in Fig. 6.

Near the central region between two consecutive electrodes a lower concentration of particles is simulated by MST with respect to the standard approximation. In the standard DEP method the particles tend to reach the bottom of the channel, while in MST case appears a zone where the particles seem to be rejected: that is confirmed by the plot of the concentration as a function of the time (Fig. 6). In all the positions evaluated, the concentration of MDA obtained with the MST method is lower than the estimated by the standard DEP theory.

The LYM case is reported in Figs. 7 and 8 considering the same type of analysis used for MDAs.

Due to the strong repulsion at the electrode edge, it is not possible to evidence a clear difference between two methods comparing the density fields only. However the time dependent density plots of the influence of aDEP is largely visible above the electrode center. In this case the rare cells which are not repelled by the electrode edge could be attracted by the electrode in the aDEP zone. We note that if compared with the other portions of the channel, where the aDEP effects are almost null, we cannot evidence substantial differences between standard DEP and MST.

The graphics in Fig. 9 show a general scenario of this behavior.

5. Conclusion

In this paper, we have studied the aDEP effects simulating the global behavior of MDA and LYM cells inside a channel with interdigitate electrodes. We obtained differences between the evaluation of DEP forces for standard and MST methods, which are strong only in limited zone of the FFF-DEP devices. It was also possible to evaluate the changes in the kinetics of the particle density field combining the electromagnetic simulations with a drift/diffusion model. The presence of aDEP could hinder the particle separation moving away MDA in pDEP and attracting LYM in nDEP.

Acknowledgment

The research is partially supported by: PO FSE Sicilia 2007–2013, 'Formazione di ricercatori altamente qualificati per l'Imaging e la Sensoristica Biomedica' CIP:2007.IT.051.PO.003/IV/L/F/9.2/0019.

References

[1] A. La Magna, M. Camarda, I. Deretzis, G. Fisicaro, S. Coffa, Coupled Monte Carlo–Poisson method for the simulation of particle–particle effects in dielectrophoretic devices, Appl. Phys. Lett. 100 (2012) 134104.

[2] Nuttawut Lewpiriyawong, Chun Yang, Dielectrophoresis field-flow fractionation for continuous-flow separation of particles and cells in microfluidic devices, Advances in Transport Phenomena 2011, pp. 29–62.

[3] Massimo Camarda, Silvia Scalese, Antonino La Magna, Analysis of the role of the particle–wall interaction on the separation efficiencies of field flow fractionation dielectrophoretic devices, ElectrophoresisWiley Online Library, 2014 http://dx.doi.org/10.1002/elps.201400385.

[4] O.E. Nicotra, La Magna, S. Coffa, A mean field approach to many-particles effects in dielectrophoresis, Appl. Phys. Lett. 93 (2008) 193902, http://dx.doi.org/10.1063/1.3025840.

[5] Fredrik Aldaeus, Yuan Lin, Johan Roeraade, Gustav Amberg, Superpositioned dielectrophoresis for enhanced trapping efficiency, Electrophoresis 26 (2005) 4252–4259.

[6] O.E. Nicotra, La Magna, S. Coffa, Particle-chain formation in a dc dielectrophoretic trap; a reaction–diffusion approach, Appl. Phys. Lett. 95 (2009) 073702, http://dx.doi.org/10.1063/1.3177332.